

Scanning tunneling microscopy and spectroscopy of Se and Te nanorods

Ujjal K. Gautam^{a,b}, Gautam Gundiah^a, G.U. Kulkarni^{a,*}

^a*Chemistry and Physics of Materials Unit, CSIR Centre of Excellence in Chemistry, Jawaharlal Nehru Centre for Advanced Scientific Research, Jakkur P.O., Bangalore 560 064, India*

^b*Solid State and Structural Chemistry Unit, Indian Institute of Science, Bangalore 450012, India*

Abstract

Se and Te nanorods obtained by a self-seeding solution growth process have been examined by scanning tunneling microscopy and spectroscopy (STM/STS). The diameters of the rods, as revealed by STM images were in the range of 10–60 nm, with aspect ratios of 10–20. The I - V data of the Se and Te nanorods exhibit band gaps of ~ 1.3 and ~ 0.4 eV, respectively, nearly independent of the diameter, and these values are close to the bulk values of Se and Te. In both the cases, the nanorods possess a small but finite conductance even in the band gap regions, the conductance value increasing with the diameter of the rod. A tunneling mechanism involving the surface states is proposed to explain this phenomenon.

PACS: 73.63. – b; 73.21.Hb; 73.20.At

Keywords: A. Nanostructures; C. Scanning tunneling microscopy and spectroscopy; D. Electronic transport

1. Introduction

One-dimensional (1D) nanostructures such as nanorods and nanotubes have been currently the subject matter of intense research due to their forthcoming applications in the field of nanoscale electronics [1–4]. Among the semiconductor materials, Se and Te deserve attention because of their interesting optical, catalytic and electronic properties [5–7]. Nanorods and other 1D nanostructures of Se and Te have been readily prepared by several solution based routes [8–11]. Recently, Rao and co-workers from this laboratory reported 1D nanostructures of Se and Te obtained by a self-seeding solution process involving the disproportionation of NaHSe and NaHTe prepared by the reaction of Se and Te with NaBH_4 , respectively [12,13]. The nanostructures synthesized by various methods need to be characterized

thoroughly in order to use them successfully in applications. In an effort to characterize the Se and Te nanostructures, we have employed scanning tunneling spectroscopy (STS), as it provides an excellent means to study the electronic transport properties. STS measurements have been used to probe the quantum size effect of CdSe nanorods [14]. ZnO nanorods of diameter 200 nm have been studied by STS to reveal the band gap of the material as well as the deep level states related to surface defects [15]. In this work, we present electronic characterization of Se and Te nanorods using STS measurements at room temperature. An analysis of the I - V characteristics has revealed that the nanorods possess band gaps close to the bulk value. In addition, we observe finite tunneling currents in the band gap regions attributable to the surface conduction states.

2. Experimental

Se and Te nanorods used in the study were synthesized

* Corresponding author. Fax: +91 80 220 827 66.
E-mail address: kulkarni@jncasr.ac.in (G.U. Kulkarni).

by a solution-based method as reported previously [12,13]. In brief, selenium powder dispersed in water was reacted with NaBH_4 under inert atmosphere to yield sodium hydrogen selenide. Sodium hydrogen selenide undergoes spontaneous disproportionation yielding amorphous selenium, which slowly dissolves and recrystallizes as t-Se nanorods. The same procedure was employed for Te nanorods also. Highly oriented pyrolytic graphite (HOPG) was used as the substrate to deposit nanorods. HOPG substrates were prepared by peeling the upper layers with an adhesive tape. The nanorod suspension in water was sonicated for 60 min, after which a drop was deposited on the substrate. The substrate was left in air but covered, for a period of 12–14 h for drying. Imaging and spectroscopy were carried out using Au (electrochemically etched) tips. The STM and STS studies were carried out at room temperature (using an Omicron Vakumphysik STS) operated in air. Lattice images and HOPG steps were used as internal calibration standards. Current–voltage (I – V) data were collected in the spectroscopy mode with the feedback loop turned off. Spectroscopy measurements were made by averaging 8–10 I – V curves at various locations on individual nanorods. Frequently, I – V data from clean areas of the HOPG substrate were collected as reference to ensure reliability of the measurements.

3. Results and discussion

Representative transmission electron microscope (TEM) images of Se and Te nanorods are shown in Fig. 1. The image of the Se nanostructures in Fig. 1(a) contains rods with diameters in the range of 50–100 nm and lengths ~ 500 nm. The image also reveals the presence of nanorods with much smaller diameter (40 nm), though less in

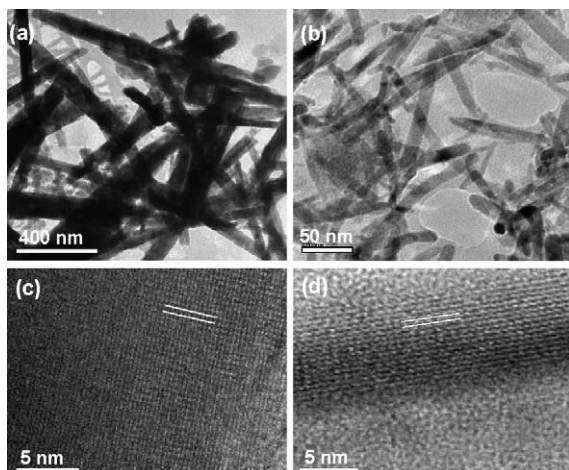


Fig. 1. TEM images of (a) Se and (b) Te nanorods. High resolution images of individual nanorods are shown in (c) and (d), respectively.

numbers. The high resolution image shown in Fig. 1(c) shows that the rods are essentially single crystalline and are devoid of any crystallographic defects. The lattice spacing of 4.9 \AA along the rod matches the separation between the (001) lattice planes of Se (JCPDF No. 06-0362), showing thereby that the growth direction is along the c -axis. Typical TEM images of the Te nanorods are presented in Fig. 1(b). The nanorods are 15–30 nm in diameter having lengths of ~ 200 nm. The image of a single nanorod is shown in Fig. 1(d), with an interlayer spacing of 3.9 \AA corresponding to $d(100)$ of hexagonal Te (JCPDF No. 36-1452).

Fig. 2 shows scanning tunneling microscope (STM) image of Se nanorods with diameters of 17 and 41 nm as measured from their z -profiles. The nanorods have small aspect ratios in the range of 10–20. However, the nanorods in the images are visibly different from the steps of HOPG (also seen in the image). Since, it is necessary not to confuse the nanostructures with the steps of HOPG, we have chosen

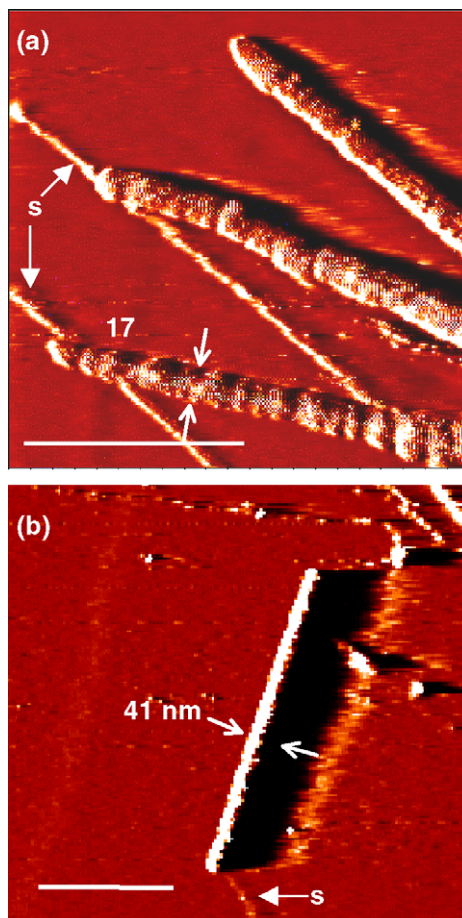


Fig. 2. STM images of Se nanorods (a) 17 nm (b) 41 nm. The images were acquired at 0.2 V bias voltage and 1 nA tunneling current. S denotes steps on HOPG. The length of the scale bars correspond to 100 nm.

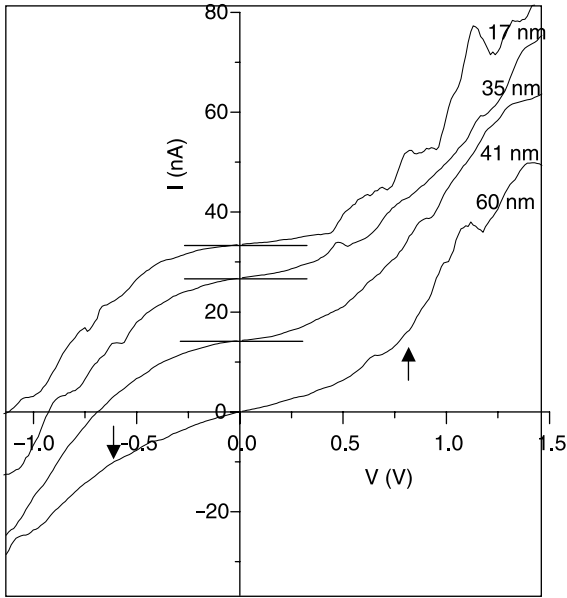


Fig. 3. I - V data for Se nanorods of various diameters. The curves are given offsets for clarity. The arrows indicate the estimated band-gap. to ignore the rod-like features whose ends were not distinctly visible.

The I - V curves obtained from four different Se nanorods with diameters of 17, 35, 41 and 60 nm are shown in Fig. 3. All the curves contain a region near zero bias, where the tunnel current is relatively small. Beyond this region, we see an abrupt increase in the tunnel current as the bias voltage is increased. For instance, in case of the 60 nm rod, there is a distinct change in the slope around bias voltage of ± 0.7 eV. This value roughly corresponds to the bulk Se band gap of 1.3 eV [8]. All the nanorods exhibited similar features, the small differences observed are perhaps due to the differences in the local density of states (LDOS). Nanostructures obtained from solution routes are usually associated with defects on the surface that can alter the LDOS to some extent. Such defects can also lend alternative pathways for electron conduction [16]. We observe from Fig. 3 that the slope of the curve near zero bias increases with increasing size of the nanorod implying an increase in the tunneling conductance. In addition, the I - V curves are characterized by features such as negative differential resistance (NDR). For example, nanorods with diameters 17 and 60 nm show distinct NDR features at ~ 1.20 V. These features were reproducible on a given nanorod, although not every rod we examined showed similar behavior. However, smaller features present at $+0.65$ and -1.04 could be seen in all the nanorods. Further work is necessary in order to understand such spectroscopy features.

In Fig. 4, we show typical STM images of three Te nanorods with diameters of 10, 15 and 28 nm. The corresponding I - V data obtained are shown in Fig. 5. The curves shown were actually calculated from the average of

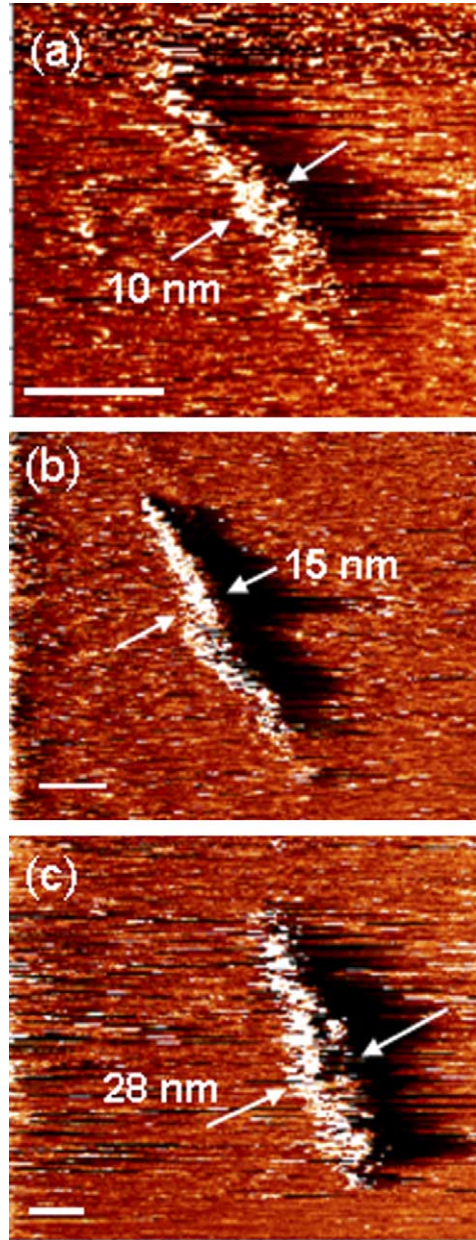


Fig. 4. STM images of Te nanorods (a) 10 nm (b) 15 nm and (c) 28 nm. The images were acquired at 0.2 V bias voltage and 1 nA tunneling current. The length of the scale bars correspond to 20 nm.

the several I - V measurements acquired at various locations of a single nanorod. It can be seen from Fig. 5(a) that the I - V curves are smooth and relatively featureless as compared to the Se counterparts in Fig. 3. Due to the small band-gap of Te (0.4 eV) [8], impurity states may be smaller in number in the gap region, resulting in smoother I - V curves. As in the case of Se nanorods, Te nanorods also show an increase in tunnel current with increasing diameter of the rods (Fig. 5) near zero bias.

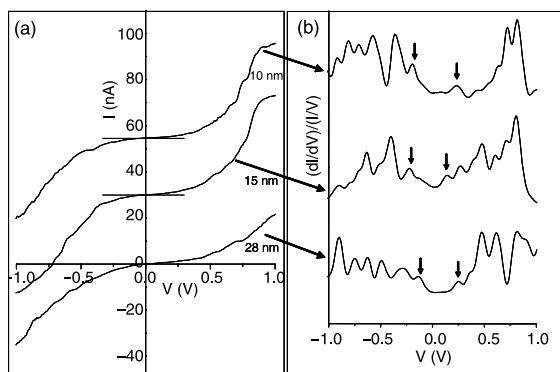


Fig. 5. (a) I - V data for Te nanorods of various diameters. The curves are given offsets for clarity. (b) Normalized conductance plots. Arrows indicate the band-gap region.

We carried out a derivative analysis of the I - V data to see if a band gap is manifested in them. Normalized conductance values which essentially represent the local density of states (LDOS) [16,17] are plotted against energy in Fig. 5(b). As can be seen from the plot, all the nanorods have features that can be related to the band-gap of tellurium. For example, in case of the 10 nm rod, we see features at $+0.23$ and -0.20 eV, standing at the band edges and thus giving a value of 0.43 eV for the band gap which is close to that of the bulk. Similar features are seen in all the nanorods. Band-gap values obtained for the 15 and 28 nm rods were 0.37 and 0.38 eV, respectively.

The properties of Se and Te nanorods examined by us are reminiscent of their bulk behavior. In particular, the band-gap values obtained from the I - V data match closely those of the bulk values. In other words, the thinnest rods examined in this study (~ 10 nm) are large enough to adopt the bulk band structure. Quantum size effects may become discernable in rods of a much smaller diameter.

What is interesting is that the nanorods exhibit non-zero tunnel current at bias voltages within the band gap (Figs. 3 and 5). Moreover, the conductance estimated from these regions seems to depend on the diameter of the rods as mentioned earlier. Fig. 6 depicts a plot of tunnel conductance (near zero bias) against the diameter for both Se and Te nanorods. Despite the different band-gaps, conductance values for Se and Te are comparable and show a monotonic increase with the rod diameter. It is possible that surface tunneling states are largely contributing to the conduction in the designated band-gap region. In rods of smaller diameters, the surface density of states are likely to be more localized owing to their higher curvatures.

Acknowledgements

We thank Prof C. N. R. Rao, FRS for suggesting the problem and helpful discussions.

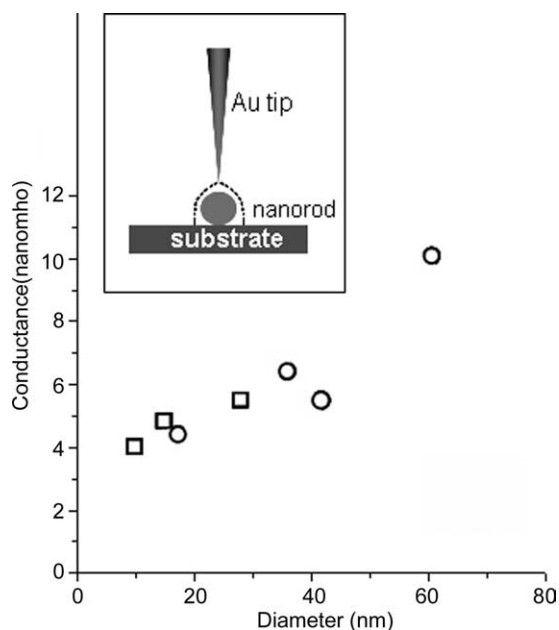


Fig. 6. Variation in the slope of the I - V curves versus the diameter of the nanorods of Se (circles) and Te (squares). Inset shows the schematic of a surface tunneling process.

References

- [1] C.N.R. Rao, F.L. Deepak, G. Gundiah, A. Govindaraj, Prog. Solid State Chem. 31 (2003) 5.
- [2] M.H. Huang, S. Mao, H. Feick, H. Yan, Y. Wu, H. Kind, E. Weber, R. Russo, P. Yang, Science 292 (2001) 1897.
- [3] X. Duan, Y. Huang, Y. Cui, J. Wang, C.M. Lieber, Nature 409 (2001) 66.
- [4] G. Klimeck, R. Lake, R.C. Brown, W.R. Bowen, W.R. Frensley, Appl. Phys. Lett. 67 (1995) 2338.
- [5] R.A. Zingaro, W.C. Cooper (Eds.), Selenium, Van Nostrand Reinhold, New York, 1974.
- [6] E. Gerlach, P. Grosse (Eds.), The Physics of Selenium and Tellurium, Springer, Berlin, 1979.
- [7] E.D. Cooper, Tellurium, Van Nostrand Reinhold Co., New York, 1974.
- [8] B. Gates, B. Mayers, B. Cattle, Y. Xia, Adv. Funct. Mater. 12 (2002) 219.
- [9] A. Abdelouas, W.L. Gong, W. Lutze, J.A. Shelnut, R. Franco, I. Moura, Chem. Mater. 12 (2000) 1510.
- [10] Q. Lu, F. Gao, S. Komarnani, Adv. Mater. 16 (2004) 1629.
- [11] B. Mayers, Y. Xia, Adv. Mater. 14 (2002) 279.
- [12] U.K. Gautam, M. Nath, C.N.R. Rao, J. Mater. Chem. 13 (2003) 2845.
- [13] U.K. Gautam, C.N.R. Rao, J. Mater. Chem. 14 (2004) 2530.
- [14] O. Millo, D. Karz, D. Steiner, E. Rothenberg, T. Mokari, M. Kazes, U. Banin, Nanotechnology 15 (2004) 1.
- [15] M.H. Zaldívar, J.V. Benavides, U. Pal, Opt. Mater. 27 (2005) 1276.
- [16] D.A. Bonnell (Ed.), Scanning Tunneling Microscopy and Spectroscopy: Theory, Techniques and Applications, VCH, New York, 1993.
- [17] N.D. Lang, Phys. Rev. B 34 (1986) 5947.